HiSST: 3rd International Conference on
High-Speed Vehicle Science Technology

14 -19 April 2024, Busan, Korea

Preliminary thermal assessment of an air-launched propelled hypersonic experimental vehicle

R. Scigliano[1], M. Marini[2], S. Di Benedetto[3], M. Albano[4], G. Ranuzzi[5]

Abstract

In the last decade, international community has shown an increasing interest in civil high-speed aviation. In particular, several studies have been carried out to assess the technical possibility of hypersonic civil flights paying attention at technical, environmental and economic viability in combination with human factors, social acceptance, implementation and operational aspects. In the past years, some innovative high-speed aircraft configurations have been proposed as results of dedicated multi-disciplinary and highly integrated design concept where aerothermodynamic, structural and propulsive issues are evaluated together in the frame of European Commission-supported research projects such as: LAPCAT I/II [1-3], ATLLAS I/II [4], HIKARI, HEXAFLY [5], HEXAFLY-International [6], STRATOFLY [7, 8, 9, 10].

In this context, starting from an in-depth investigation of the status of past and on-going activities, CIRA has launched a national project funded by PRO.R.A. (Aerospace Research Program), aiming at designing, manufacturing and flight-testing a propelled hypersonic demonstrator, namely the Scramjet Hypersonic Experimental Vehicle (SHEV) [11]. The Italian Space Agency (ASI) is also funding the activities for a three-year period. This paper focuses the attention on the preliminary thermal assessment of the experimental flight vehicle mainly from the structure and material point of view.

Keywords: *hypersonic, thermal analysis, material layout, FEM*

Nomenclature

T	Temperature.	q	Heat flux rate per unit area
T_w	Wall temperature	σ	Stefan Boltzmann constant
T_0	Stagnation point temperature	ε	Emissivity
h	Convective heat coefficient		

1. Introduction

Over the last years, innovative concepts of civil high-speed transportation vehicles were proposed [1-10]. These vehicles have a strong potential to increase the cruise range efficiency at high Mach numbers, thanks to efficient propulsion units combined with high-lifting vehicle concepts. In this framework, manufacturing a propelled hypersonic demonstrator would represent for Italy the opportunity to play a central role as well as the chance to improve the technical skills in terms of designing hypersonic as well as re-entry and suborbital vehicles. For this reason, CIRA and ASI have co-funded a national project aiming at designing a propelled hypersonic demonstrator, namely the Scramjet Hypersonic Experimental Vehicle (SHEV).

The project has the aim of improving the state-of-the art by preliminary designing a small scale hypersonic propelled demonstrator.

---

[1] *Italian Aerospace Research Centre (CIRA), Via Maiorise snc, 81043 Capua, Italy, Email: r.scigliano@cira.it*

[2] *Italian Aerospace Research Centre (CIRA), Via Maiorise snc, 81043 Capua, Italy, Email: m.marini@cira.it*

[3] *Italian Aerospace Research Centre (CIRA), Via Maiorise snc, 81043 Capua, Italy, Email: s.dibenedetto@cira.it*

[4] *ASI, Agenzia Spaziale Italiana, 00133 Rome, Italy, marta.albano@asi.it*

[5] *ASI, Agenzia Spaziale Italiana, 00133 Rome, Italy, giuliano.ranuzzi@asi.it*

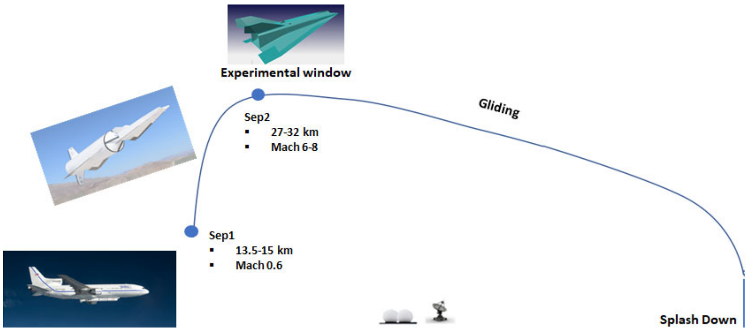

Fig 1. SHEV mission profile.

This paper describes the overall numerical tradeoff that led to a preliminary vehicle material layout. In particular, a preliminary mission definition has been performed evaluating the advantages and the drawbacks of a ground-launched vs air-launched missions. The first solution presents the advantage of a well-established know-how [5;6] but has the big disadvantage of having elevated costs and few launchpads available across Europe. For all these reasons, an air-launched mission (a carrier aircraft, a launch vehicle and the SHEV (Fig 1) profile with a preliminary trajectory has been considered and the following high-level requirements have been defined:

- Class vehicle: length 4.5 m, mass 1100÷1200 kg.
- Flight regime: Mach = 6÷8, trimmed and stable at constant height 28÷32 km.
- Aero-propulsive balance with positive aerodynamic efficiency L/D=3÷4.
- Airbreathing scramjet hydrogen propulsive system working for a minimum time of 10 s.

Thus, starting from a preliminary "waverider" layout configuration (Fig 2), different thermal analysis on the main structure, according to the aerothermal input coming from proper CFD steady simulations, that are out of the scope of this paper, have been performed on a preliminary trajectory, with the main goal of selecting the material layout for the SHEV main structural components.

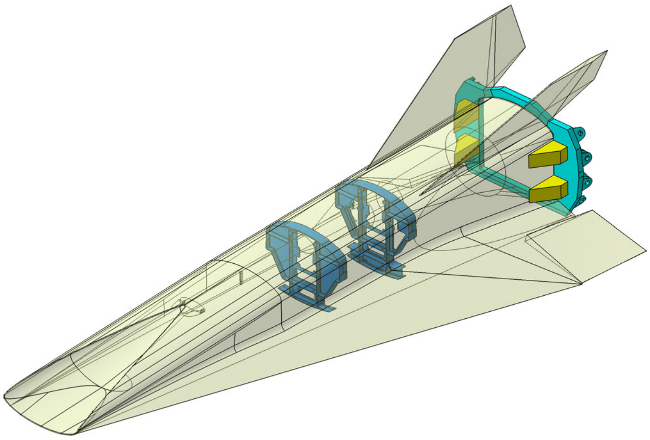

Fig 2. SHEV fuselage structure.

2. Thermal Analysis

2.1. Numerical method

A preliminary extensive transient thermal analysis numerical campaign has been performed. The thermal behaviour of the vehicle has been assessed by means of the FE method implemented in the software ANSYS® [12]. A transient thermal analysis along the reference trajectory has been performed to evaluate the time dependent temperature of the structure. The implemented numerical procedure is schematically reported in Fig 3.

In particular:

- The available CAD configuration of the vehicle is implemented in Ansys Workbench, and properly modified, if required.
- The computational 3D mesh is generated and is composed by about 1.1 million nodes and 315k 3D HEXA elements. (Fig 4)
- Steady CFD calculations [13] have been realized in a certain number of flight conditions along the considered trajectory to evaluate the convective heat transfer coefficient spatial distributions over the vehicle surface, see Fig 5.

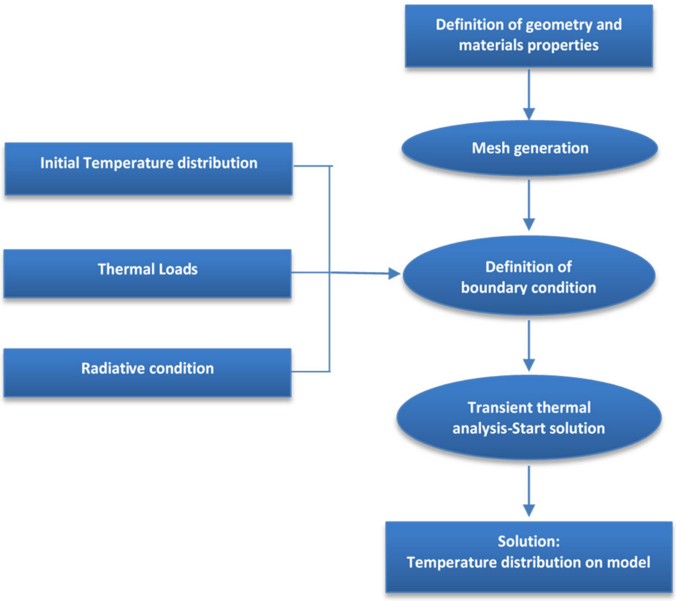

Fig 3. Thermal transient numerical procedure flow chart.

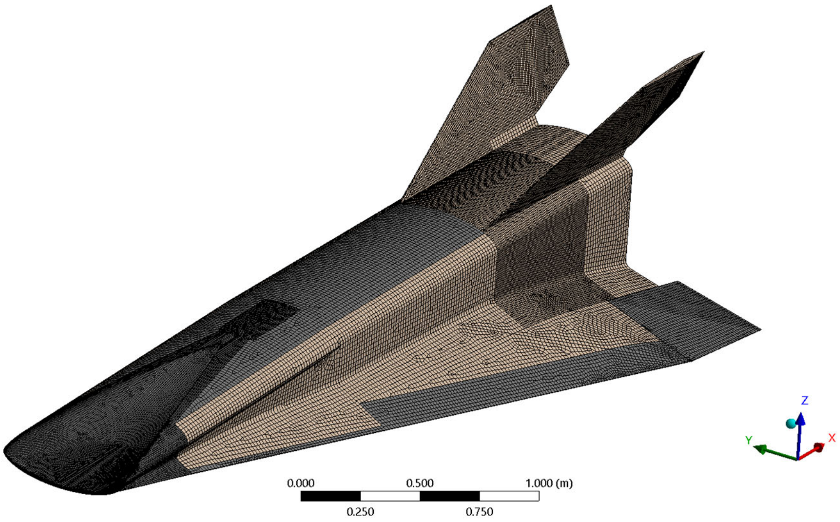

Fig 4. SHEV 3D mesh.

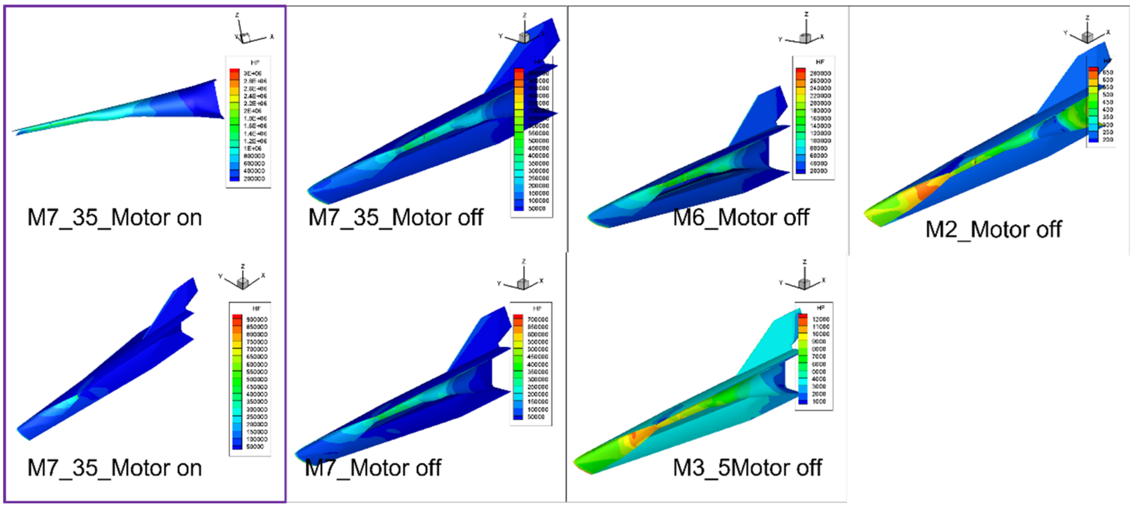

Fig 5. CFD simulations at different Mach numbers.

- The flight trajectory has been then split in a certain number of legs, each of them characterized by a specific flight condition previously analyzed by CFD (effect of angle of attack, Mach number and Reynolds number are therefore considered).
  For each trajectory leg, the heat transfer coefficient distributions are properly scaled by the stagnation-point heat transfer coefficient variation along the selected trajectory leg, normalized with respect to the corresponding reference condition (i.e., the flight condition analyzed by CFD). Referring to the nomenclature reported in Fig 6, Eq. 1 is applied.

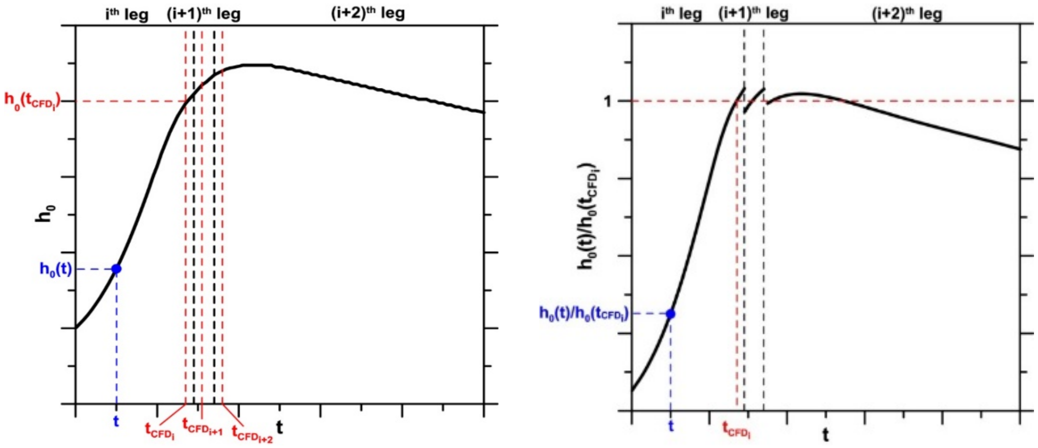

a) b)

Fig 6. CFD results scaling along the trajectory.

$$h(x,t) = h(x)|_{CFD_i} \cdot \frac{h_0(t)}{h_0(t_{CFD_i})} \qquad (1)$$

An exemplary plot of the normalized stagnation-point heat transfer function, piecewise defined in each trajectory leg, is shown in Fig 6b. In particular, the stagnation-point convective heat transfer coefficient is estimated by scaling the hot wall stagnation-point convective heat flux variation along the trajectory by the stagnation temperature profile, as reported in Eq.2.

$$h_0 = \frac{\dot{q}_{0,hw}}{T_0} \qquad (2)$$

In turn, the hot wall stagnation-point convective heat flux variation along the trajectory is evaluated according to the well-known Zoby's formulation. The transient thermal analysis is then set assuming, as convective boundary condition, the heat transfer coefficient evaluated according to the previously discussed procedure and the total temperature (T_0) profile along the flight (in coherence with the CFD modelling) (Fig 7). A radiative equilibrium condition is also considered for all the external surfaces. Therefore, the overall condition reported in Eq. 3 is applied.

$$\dot{q} = h \cdot (T_0 - T_w) - \sigma \cdot \varepsilon \cdot T_w^4 \qquad (3)$$

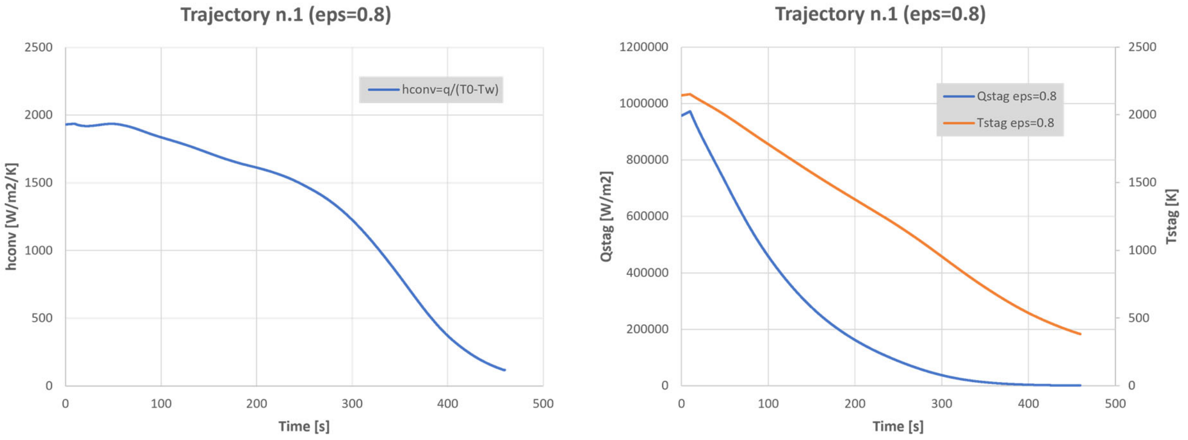

Fig 7. Heat transfer coefficient (left) and stagnation-point heat flux and total temperature (right) along the trajectory.

- Finally, correct boundary conditions must be set in terms of radiative conditions (Fig 8), i.e. the proper surface emissivity is set for external panels, CMC parts and combustion chamber components.

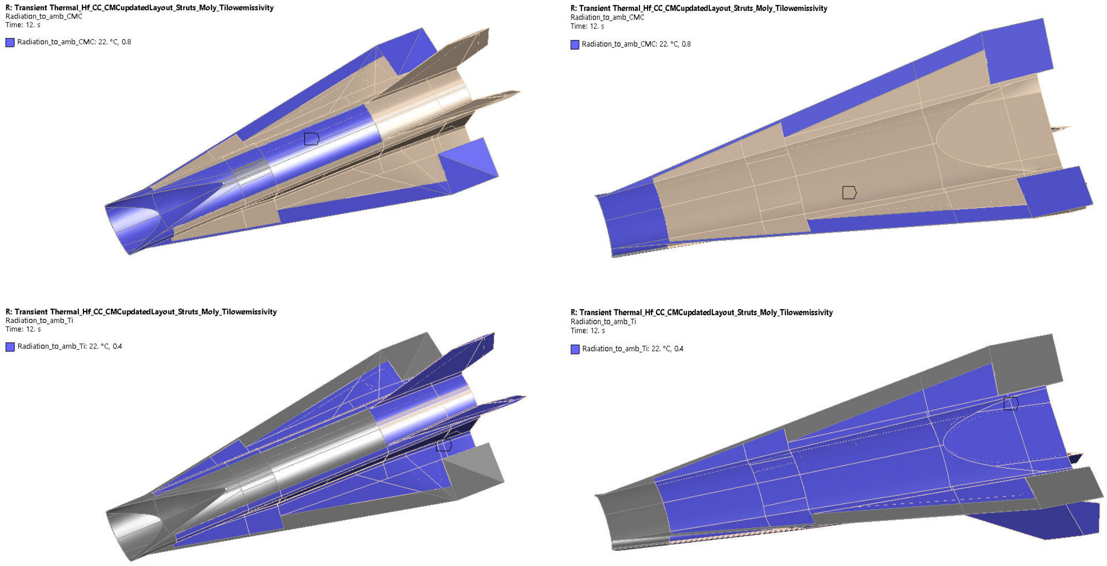

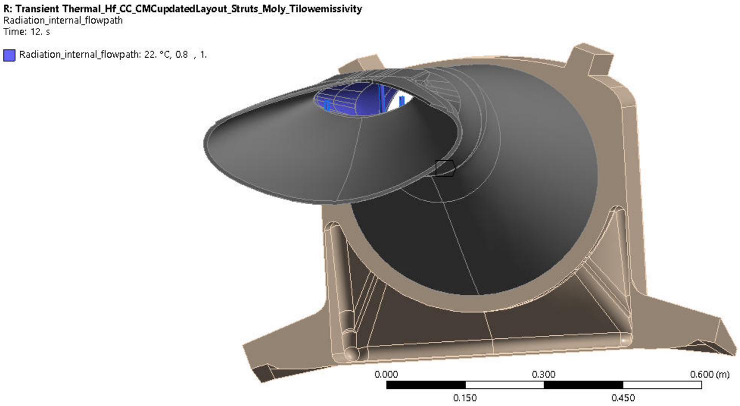

Fig 8. Radiative conditions on different SHEV surfaces.

- Temperature distributions in function of time for the overall structure are computed as output of the present thermal analysis.

2.2. Main results

Several transient thermal analyses have been performed. Finally, 7 different FEM with different material layouts and distributions have been developed**,** and the main criticalities have been highlighted and overcome either by changing material or by changing the material layout. This iterative approach has led us to go through an optimal thermal distribution.

Table 1 summarizes the different material distribution w.r.t the different main structural components.

Table 1. Different FEM material layout

	Model 1	**Model 2**	**Model 3**	**Model 4**	**Model 5**	**Model 6**	**Model 7**
Component	**Material**	**Material**	**Material**	**Material**	**Material**	**Material**	**Material**
Hot structure	CMC (ISiComp®)	CMC (ISiComp®)	CMC (ISiComp®)	CMC (ISiComp®)	CMC (ISiComp®)	CMC (ISiComp®)	CMC (ISiComp®)
Cold structure	Ti6Al4V	Ti6Al4V	Ti6Al4V	Ti6Al4V	Ti6Al4V	Ti6Al4V (ε=0.4)	Ti6Al4V (ε=0.4)
Propulsive flow path	CMC (ISiComp®)	CMC (ISiComp®)	CMC (ISiComp®)	CMC (ISiComp®)	CMC (ISiComp®)	CMC (ISiComp®)	CMC (ISiComp®)
Frames	Ti6Al4V	CMC (ISiComp®)	CMC (ISiComp®)	CMC (ISiComp®)	CMC (ISiComp®)	CMC (ISiComp®)	CMC (ISiComp®)
Struts	CMC (ISiComp®)	CMC (ISiComp®)	CuZr	Molybden	CuZr	CuZr	Molybden
Fins	Ti6Al4V	Ti6Al4V	Ti6Al4V	Ti6Al4V	Ti6Al4V	Ti6Al4V	Ti6Al4V

In particular, the set of structural external parts, where the use of high temperature materials is needed, is indicated as hot structure. It includes: flaps, wing leading edges, intake, external part of propulsive duct. The remaining external parts belong to the cold structure subsystem. Fig 9 shows the material distribution of model 7, i.e. the model that leads to the most satisfying results on the thermal point of view as summarized in Fig 10 to Fig 13 where the thermal map for the different material / components are depicted at the most critical time instant along the trajectory.

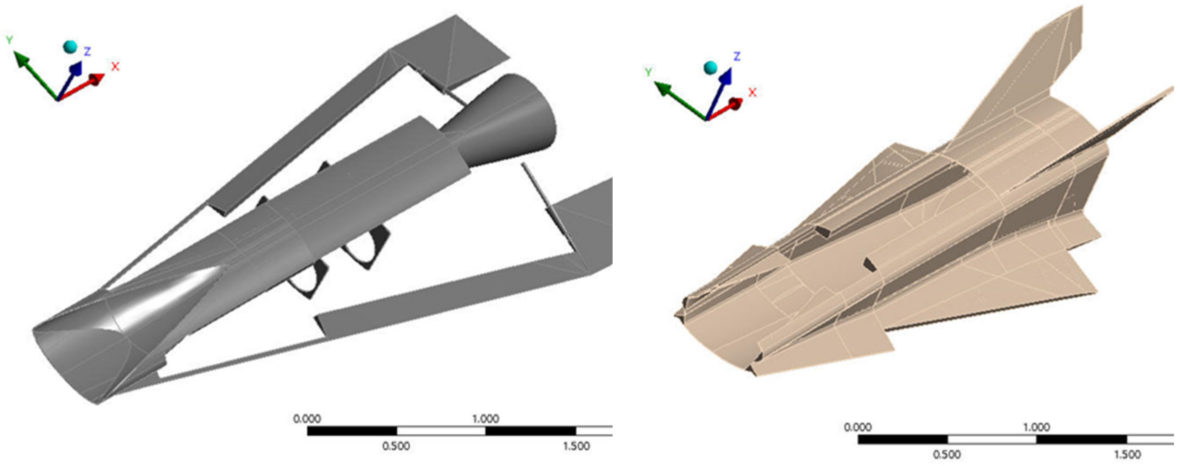

SHEV ISiComp ® components

SHEV Titanium components

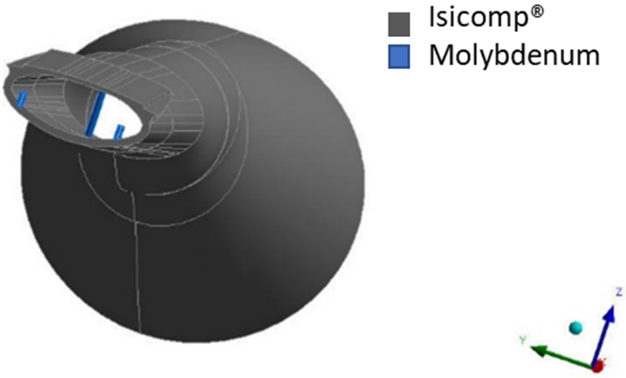

SHEV Molybdenum struts in the combustion chamber

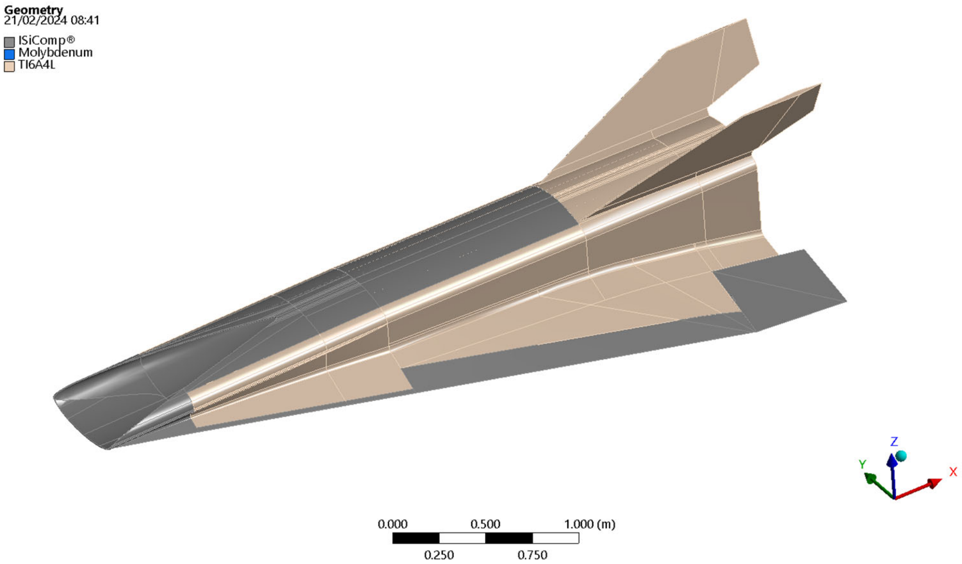

Fig 9. SHEV Material layout.

In particular, Fig 10 shows the thermal map of the CMC main structural components highlighting how the hottest spot is in the crotch area and it occurs after 20 seconds, where a temperature of about 1490°C is expected. Anyhow, this value is widely under the ISiComp® allowable, i.e., over 1600°C.

Results are slightly different for the propulsive flowpath (Fig 11) where a maximum temperature value of 1645°C is predicted at the interface between the struts and the duct wall at the end of the propulsive phase (motor-on phase lasts 10 seconds). This value is acceptable because it lasts only few seconds and it deals with an internal point in which no oxidation phenomena occur. At the same time instant the thermal map of the three struts is shown in Fig 12 where a maximum temperature of about 1818 °C is computed. This value is under the molybdenum service temperature (range is between 1900°C – 2226°C).

Finally, Fig 13 shows the Ti6Al4V components thermal maps at the metal most critical instant, i.e., at t =90s. As clearly depicted in the figure, the structure withstands the thermal environment, being the computed temperatures under the maximum service temperature of 600°C everywhere excepted at vertical fin leading edges where in a narrow area of 1.5 cm a maximum value of 927°C is computed. This value could be acceptable because that narrow area is not subject to high structural stresses. Anyhow, higher radii of curvature of leading edge are suggested and will be evaluated to get lower heat loads on these edges.

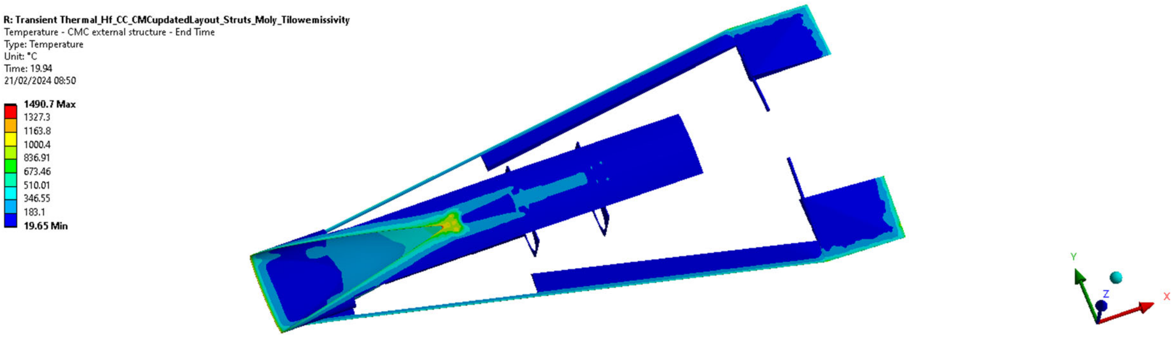

Fig 10. CMC parts (including intake) thermal result.

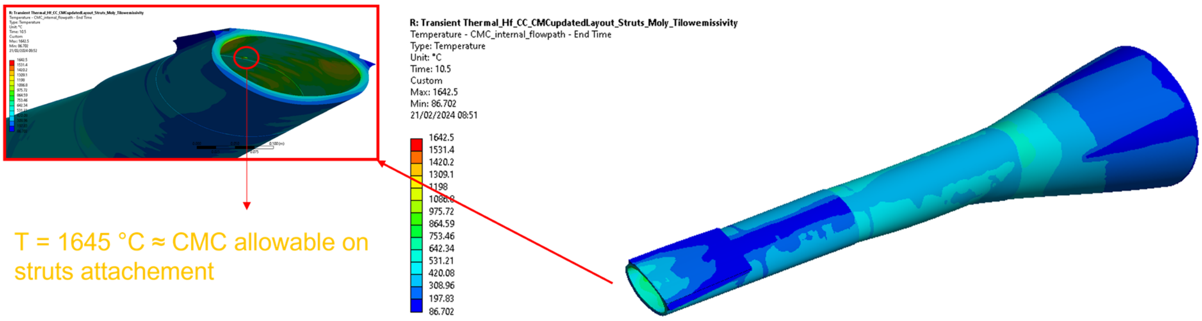

Fig 11. CMC parts internal flowpath (excluding intake) thermal result.

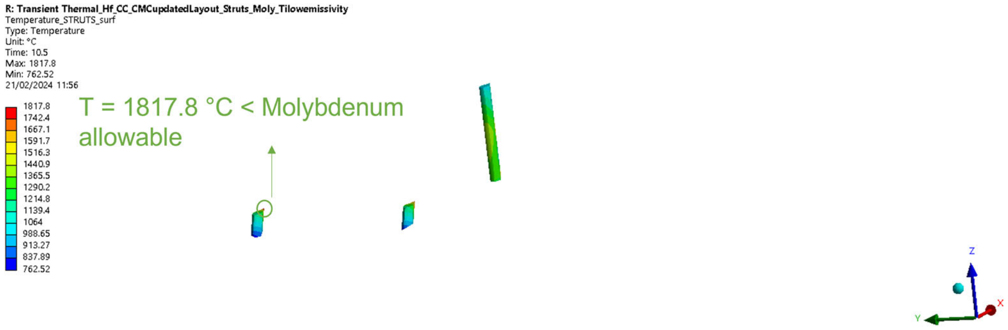

Fig 12. Molybdenum struts thermal result.

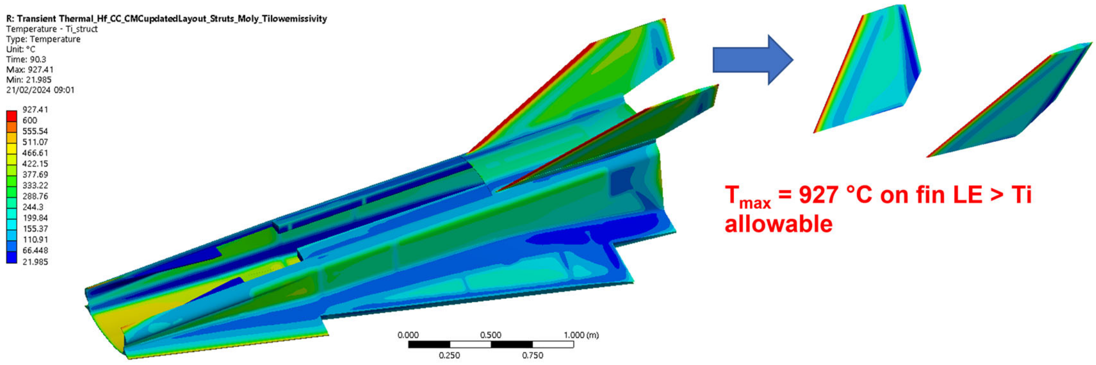

T_{max} = 927 °C on fin LE > Ti allowable

Fig 13. Ti6Al4V components thermal result.

3. Conclusions

Main conclusions of the present preliminary thermal assessment indicate that CMC can be widely employed for the main structure of SHEV vehicle, in particular for the air intake, the propulsive flow path, the internal frames, the leeward panels, the wing leading edges and the flaps. Titanium alloy could also be taken into account for leeside panels and other main components over exposed to high temperature, such as main fuselage, vertical tail as well as wing root. Nevertheless, some criticalities still remain on tail leading edges whose geometrical shape must be changed. Indeed, higher radii of curvature of leading edge are suggested to get lower heat loads in that area. Finally, struts of combustion chamber could be manufactured with molybdenum whose high strength at elevated temperature is well-adapted to the specific application. On the other hand, a proper interface attachment must be designed between the struts and the ISiComp ® internal combustion chamber wall.

In the next future, the design of the demonstrator will be updated with the outcomes of the preliminary analyses, the internal structure and the internal equipment layout will be detailed. This activity will lead to a subsequent Thermal Control System (TCS) design phase necessary to ensure equipment survivability.

A successive global thermal analysis on the full vehicle will lead to a preliminary thermo-structural design of the SHEV.

Acknowledgements

The work has been co-funded by Italian Space Agency and CIRA ScpA in the frame of the agreement nr. 2022-13-HH.0-F43D22000410005.

References

1. Steelant, J., Varvill, R., Defoort, S., Hannemann, K., Marini, M.: Achievements Obtained for Sustained Hypersonic Flight within the LAPCAT-II Project, 20th AIAA International Space Planes and Hypersonic Systems and Technologies Conference, Glasgow, Scotland, AIAA-2015-3677, 2015.
2. Steelant, J., Langener, T., Murray, N., Meerts, C., Barton, A., Mack, A.: Preliminary Mach 8 Turbo-Based/DMR Vehicle Analysis: Update of the LAPCAT MR2.4 Waverider based Vehicle, LAPCAT-II ACP7-GA-2008-211485, D3.1.9, 2014.
3. Langener, T., Steelant, J.: Trajectory Analysis for the Updated LAPCAT-MR2.4 Waverider based Vehicle, LAPCAT-II ACP7-GA-2008-211485, D3.1.9 Part E, 2013.

4. Steelant, Johan. ATLLAS: Aero-thermal loaded material investigations for high-speed vehicles. In: 15th AIAA International Space Planes and Hypersonic Systems and Technologies Conference. 2008. p. 2582.
5. Steelant J. et al., Conceptual Design of the High-Speed Propelled Experimental Flight Test Vehicle HEXAFLY, 20th AIAA International Space Planes and Hypersonic Systems and Technologies Conference, Glasgow, Scotland, AIAA 2015-3539.
6. Di Benedetto S. et al., Multidisciplinary Design and Flight Test of the HEXAFLY-INT Experimental Flight Vehicle Hexafly-Int, HiSST: International Conference on High-Speed Vehicle Science Technology, Moscow, Russia, 2018.
7. Nicole Viola, Davide Ferretto, Roberta Fusaro, Roberto Scigliano. Performance Assessment of an Integrated Environmental Control System of Civil Hypersonic Vehicle. Aerospace 2022, 9 (4), 201; https://doi.org/10.3390/aerospace9040201.
8. Roberta Fusaro, Davide Ferretto, Nicole Viola, Roberto Scigliano, Valeria De Simone, Marco Marini. Liquid Metals Heat-Pipe solution for hypersonic air-intake leading edge: Conceptual design, numerical analysis and verification. Acta Astronautica, Volume 197, 2022, Pages 336-352, ISSN 0094-5765, https://doi.org/10.1016/j.actaastro.2022.05.034.
9. R. Scigliano, V. De Simone, R. Fusaro, D. Ferretto, M. Marini, N. Viola, Cooling System Of Stratofly Hypersonic Vehicle: Conceptual Design, Numerical Analysis And Verification. 33rd Congress of the International Council of the Aeronautical Sciences 4 - 9 September 2022. Stockholm, Sweden.
10. R. Scigliano, V. De Simone, M. Marini, P. Roncioni, R. Fusaro, N. Viola. Preliminary Finite Element Thermal Analysis of STRATOFLY Hypersonic Vehicle. 23rd AIAA International Space Planes and Hypersonic Systems and Technologies Conference - AIAA HYPERSONICS 2020, March 10-12, 2020, Montreal, Quebec, Canada.
11. S. Di Benedetto, M. Marini, P. Roncioni, A. Vitale, P. Vernillo, R. Scigliano, S. Cardone, M. Albano, R. Bertacin. The Scramjet Hypersonic Experimental Vehicle. HiSST: 3rd International Conference on High-Speed Vehicle Science Technology, 14-19 April 2024, Busan, Korea.
12. ANSYS® Inc., Thermal analysis guide, Release 21.1, 2020.
13. Pietro Roncioni, Oreste Russo, Francesco Cascone, Marco Marini, Sara Di Benedetto, Marta Albano, Roberto Bertacin. Aerodynamic and Propulsive Assessment of an Experimental Hypersonic Scramjet System. HiSST: 3rd International Conference on High-Speed Vehicle Science Technology, 14-19 April 2024, Busan, Korea.